

## Next-Generation Time-Resolved Scanning Probe Microscopy

### - Ushering in a New Era of Nanoscale Exploration with Enhanced Usability

Katsuya Iwaya,<sup>1</sup> Hiroyuki Mogi,<sup>2</sup> Shoji Yoshida,<sup>2</sup> Yusuke Arashida,<sup>2</sup> Osamu Takeuchi,<sup>2</sup>  
and Hidemi Shigekawa\*<sup>2</sup>

<sup>1</sup>*UNISOKU Co., Ltd., Hirakata, Osaka 573-0131, Japan*

<sup>2</sup>*Faculty of pure and applied sciences, University of Tsukuba, Tsukuba, Ibaraki 305-8573, Japan*

(\*Electronic mail: [hidemi@ims.tsukuba.ac.jp](mailto:hidemi@ims.tsukuba.ac.jp))

(Dated: 28 March 2024)

Understanding the nanoscale carrier dynamics induced by light excitation is the key to unlocking futuristic devices and innovative functionalities in advanced materials. Optical pump-probe scanning tunneling microscopy (OPP-STM) has opened a window to these phenomena. However, mastering the combination of ultrafast pulsed lasers with STM requires high expertise and effort. We have shattered this barrier and developed a compact OPP-STM system accessible to all. This system precisely controls laser pulse timing electrically and enables stable laser irradiation on sample surfaces. Furthermore, by applying this technique to atomic force microscopy (AFM), we have captured time-resolved force signals with an exceptionally high signal-to-noise ratio. Originating from the dipole-dipole interactions, these signals provide insights into the carrier dynamics on sample surfaces, which are activated by photo-illumination. These technologies are promising as powerful tools for exploring a wide range of photoinduced phenomena in conductive and insulating materials.

## I. INTRODUCTION

The need for exceptional spatial and temporal resolutions is at the heart of deciphering the intricate carrier dynamics in nanoscale materials. Conventional scanning tunneling microscopy (STM), although providing unparalleled spatial and energy resolutions, hits a temporal resolution ceiling at sub-millisecond levels owing to preamplifier bandwidth constraints. With the integration of transformative OPP techniques into STM, such barriers have been overcome, realizing higher temporal resolutions. This fusion is pivotal in probing materials' complex nonequilibrium carrier and spin dynamics<sup>1,2</sup>. Another technique, the use of a subcycle electric field as bias voltage, has been incorporated as an electric-field-driven STM. This technique provides temporal resolutions of less than 1 ps and 30 fs, maintaining the spatial resolution of STM using terahertz (THz) and mid-infrared pulses<sup>3-6</sup>. This leap in technology widens the horizon of time-resolved STM; however, it still requires high expertise and simplification of the system to make it accessible for a broad spectrum of research endeavors. In addition, since the application of STM is limited to conducting materials, extending this OPP technique to atomic force microscopy (AFM) would further expand the capabilities of this time-resolved measurement technique.

## II. OPTICAL PUMP-PROBE SCANNING TUNNELING MICROSCOPY (OPP-STM)

In the conventional OPP method, pump light and probe light, which are delayed in time, are irradiated onto a sample, as shown in Figure 1a. When carriers such as electrons and holes excited by the pump light remain in an excited state, the excitation by the probe light is suppressed (absorption bleaching). Therefore, by measuring the reflectivity of the probe light as a function of the delay time, one can investigate the dynamics of the states excited by the pump light with a time resolution corresponding to the pulse width of the excitation light. However, the spatial resolution is limited to the diffraction and light-spot size (around micrometer order).

In OPP-STM, the sample surface under the STM tip is first excited by a pump pulse and subsequently by a probe pulse with a delay time  $t_d$ , and the tunneling current is detected using a conventional preamplifier (Fig. 1b)<sup>1</sup>. When  $t_d$  is sufficiently long ((1) in Fig. 1c), most of the photocarriers excited by the pump pulse relax to the ground state before the subsequent probe pulse illumination so that a similar number of carriers would be excited by the probe pulse as with the pump pulse, resulting in a large transient current  $I_{\text{probe}}^*$ . In contrast, when  $t_d$  is short, the excited

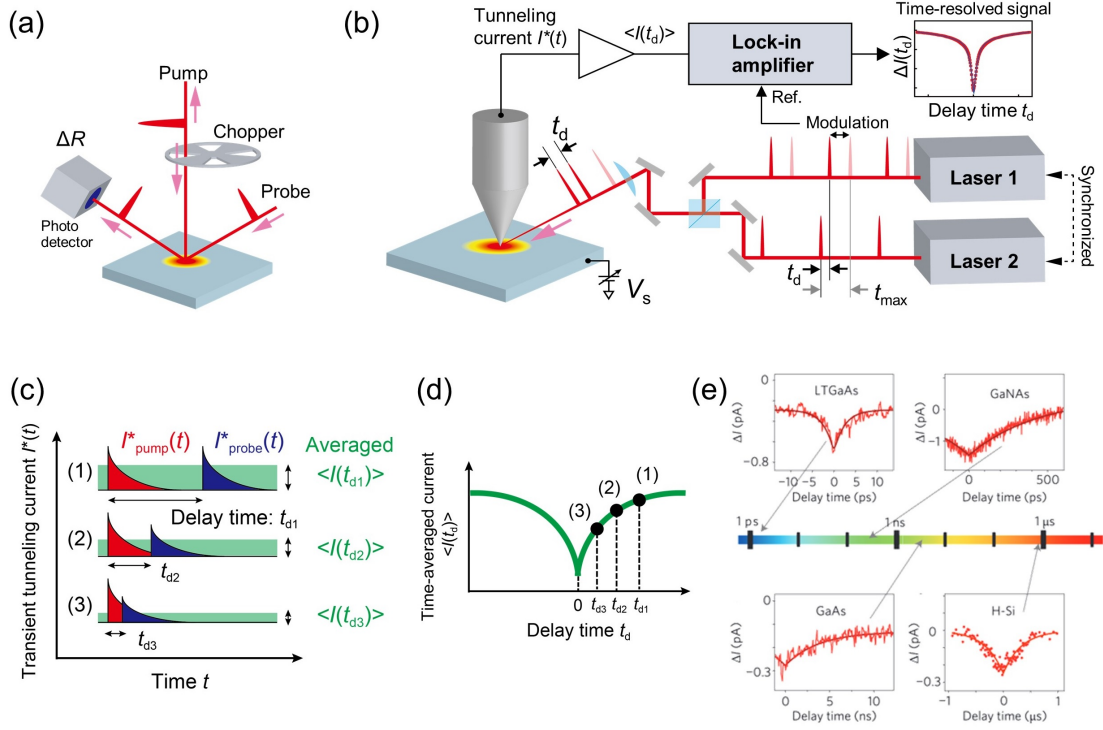


FIG. 1. (a) Conventional OPP configuration. (b) Schematic of OPP-STM with the delay-time modulation method. (c) Transient tunneling current  $I^*$  induced by the pump light and probe light at representative delay time  $t_d$ . Time-averaged tunneling current  $\langle I(t_d) \rangle$  is shown for each case (green rectangular). (d)  $\langle I \rangle$  as a function of  $t_d$ . The time-averaged  $\langle I \rangle$  corresponding to each case in (c) is plotted. (e) Time-resolved signals obtained for several samples<sup>1</sup>.

states remain occupied with the photocarriers excited by the pump pulse when the probe pulse illuminates the sample so that the optical absorption saturates, resulting in a small  $I^*_{\text{probe}}$  ((3) in Fig. 1c). By illuminating a pair of pump and probe pulses sequentially and by varying  $t_d$ , one can detect a time-averaged tunneling current  $\langle I \rangle$  as a function of  $t_d$  (Fig. 1d). By fitting the time-resolved tunneling current with an exponential function, we can obtain a decay time at the tip location, as examples are shown in Figure 1e<sup>1</sup>.

In the macroscopic OPP technique, the modulation of optical intensity is conventionally utilized to detect a weak OPP-induced signal. However, the optical intensity modulation causes severe problems, such as the thermal expansion of the STM tip. Since changes in tip-sample distance are exponentially multiplied in the tunneling current, the optical intensity modulation cannot be directly applied to STM. To suppress the thermal expansion effect, we have developed an ex-

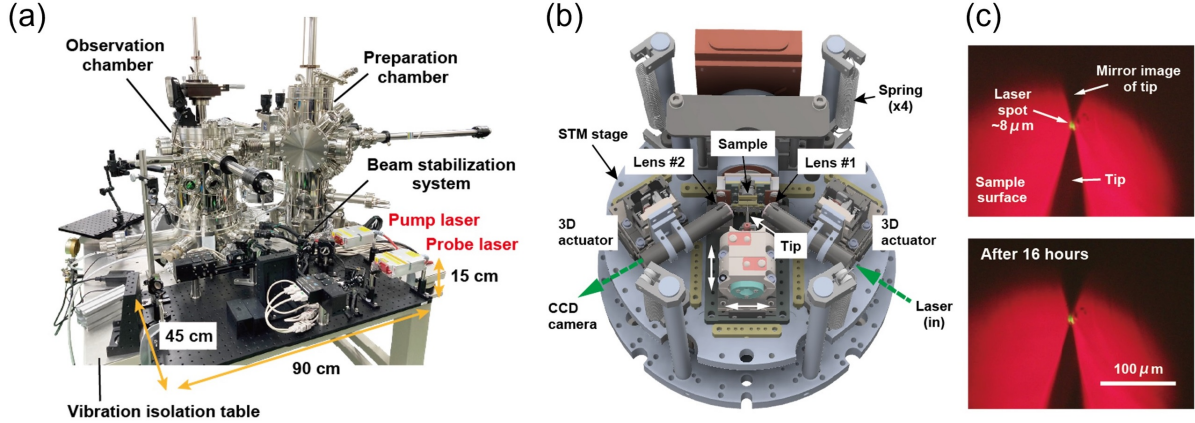


FIG. 2. (a) Photograph of the compact OPP-STM system. (b) Three-dimensional illustration of the OPP-STM unit. (c) Optical image of the tip and its mirror image on GaAs(110) surface with a laser spot illuminated at the tunneling junction before (top) and after 16 h (bottom), showing the stability of the laser spot<sup>11</sup>.

cellent delay-time modulation technique<sup>1</sup>. In this technique, we use two delay times ( $t_d$  and  $t_{\max}$  in Fig. 1b). The longer delay time  $t_{\max}$  is generally set to one-half of the laser pulse interval (for example,  $0.5 \mu\text{s}$  for 1 MHz repetition rate), corresponding to the longest delay time available for the selected repetition rate. We modulate the delay time between  $t_d$  and  $t_{\max}$  at, for example, 1 kHz and detect the resultant tunneling current  $\Delta I(t_d) = \langle I(t_d) \rangle - \langle I(t_{\max}) \rangle$  using the lock-in amplifier (Fig. 1b). This modulation technique enables us to keep the thermal load at the tunnel junction constant, substantially suppressing the thermal expansion effect.

### III. COMPACT AND STABLE OPP-STM

The delay time modulation technique has enabled reliable OPP-STM measurements. Since then, many studies such as the atomic scale carrier dynamics around a single impurity on a GaAs surface<sup>7,8</sup> and the visualization of the ultrafast carrier dynamics in a GaAs-PIN junction<sup>9</sup> have been reported. However, the optical system has been generally complex and large in scale, hindering the widespread use of this technique. To overcome this difficulty, the OPP-STM system, whose laser-pulse timing is electrically controlled by external triggers, has significantly improved the ease of use, but its temporal resolution has been limited to the nanosecond range<sup>10</sup>. In addition, fluctuations in optical intensity cause unexpected issues, such as the thermal expansion effect,

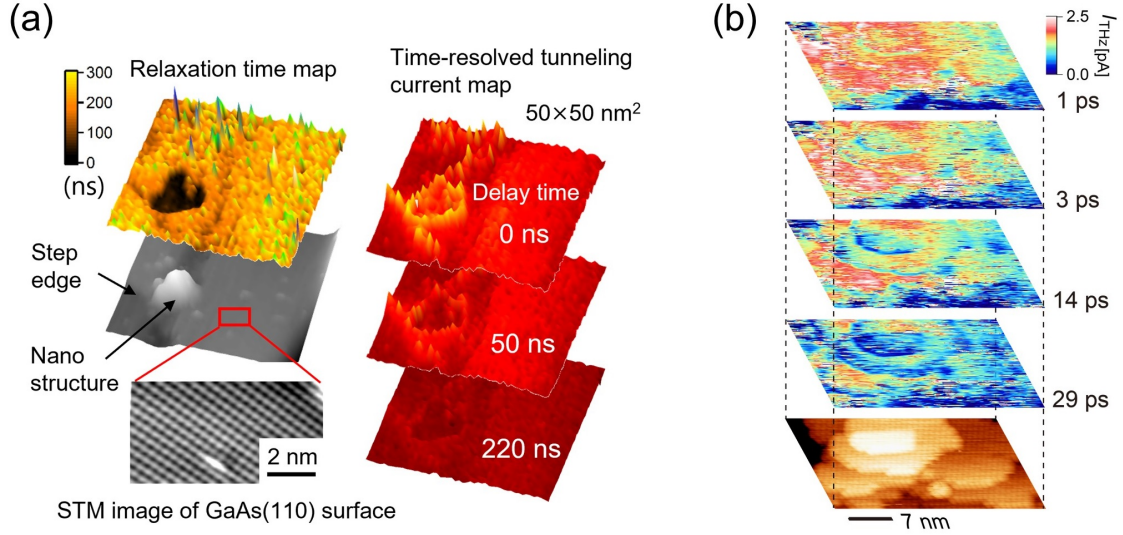


FIG. 3. (a) Grid-point time-resolved tunneling current measurement on GaAs(110) cleaved surface<sup>11</sup>. Characteristic features along the step edge and the perimeter of the nanoscale bump structure are identified in the time-resolved tunneling current map (right). By fitting a time-resolved tunneling current curve at each grid point, we can obtain the nanoscale relaxation time map (top left). (b) Snapshots of ultrafast motion of photoinjected electrons in a  $C_{60}$  multilayer/ Au sample obtained by THz-STM<sup>5</sup>.

making the accurate observation of physical phenomena challenging.

To improve the temporal resolution and the stability of laser illumination based on a compact electrically controlled laser system (Fig. 2a), the OPP-STM system with a temporal resolution of tens of picoseconds has recently been developed<sup>11</sup>. The long-term stability of laser illumination was realized also by placing the focus lens on the STM stage (Fig. 2b) and confirmed by monitoring the tip and its mirror image on the sample surface together with a laser spot focused on the tip-sample junction (Fig. 2c).

To demonstrate the performance of the system, we conducted a grid-point time-resolved tunneling current measurement on GaAs(110) surfaces at  $T = 6$  K (Fig. 3a). By measuring the time-resolved tunneling current at each grid point, we can compile the time-resolved tunneling current maps at each delay time and determine characteristic features along the nanostructure (Fig. 3a, right). Furthermore, it is possible to map a relaxation time by fitting each curve with an exponential function. The relaxation time map (Fig. 3a, top left) demonstrates that the relaxation time inside the nanoscale bump structure is substantially shorter than that of its surroundings. This mapping technique is powerful in visualizing carrier dynamics associated with nanoscale struc-

tures. Figure 3b shows an example of a time-resolved signal map obtained by THz-STM. The improvement in the usability of the optical system can be extended to electric-field-driven STM, which is currently our ongoing investigation.

#### IV. OPP ATOMIC FORCE MICROSCOPY

The optical system we have developed is also applicable to AFM, expanding its potential beyond conductive materials such as semiconductors and metals, traditionally targeted in STM. Integrating AFM into our repertoire significantly broadens the horizons of nanoscale time-resolved microscopic techniques. Previous studies have clarified the photoexcited dynamics of forces originating from surface photovoltage and dipole-dipole interactions (Fig. 4a) based on optical intensity modulation (Fig. 1a)<sup>12,13</sup>. We have advanced these achievements by combining electrically controlled delay-time modulation with tuning-fork-type frequency modulation (FM) AFM (Fig. 4b)<sup>14</sup>. By focusing optical pulse pairs onto the apex of the AFM probe, we were able to detect the amplitude of the frequency shift  $\Delta f$  as a time-resolved signal. The markedly stable time-resolved measurements on bulk WSe<sub>2</sub>, a layered semiconductor, have unveiled dynamics with two decay components through an ultrafast photoinduced force (Fig. 4c). These signals, decoded as the surface recombination and diffusion of photocarriers through tunneling current and force spectroscopy, mark a significant stride in our understanding of material properties. This innovative approach not only resolves the limitations encountered in time-resolved STM due to tunneling current but also paves the way for its application across a diverse array of materials, setting a new standard in nanoscale imaging.

#### V. CONCLUSION

Our streamlined optical system markedly eases researchers' path to harness the transformative power of the OPP-STM technique. With the multiprobe (MP) system, features such as small islands on an insulating substrate can be observed by using one tip as an electrode while conducting STM measurements with the other tip. The OPP-MP measurements have already been demonstrated on monolayer transition metal dichalcogenides to investigate nanoscale exciton dynamics<sup>15,16</sup>. Regarding the limitations of wavelength and temporal resolutions, cutting-edge laser technology, which has been rapidly developing, may overcome these limitations, thereby

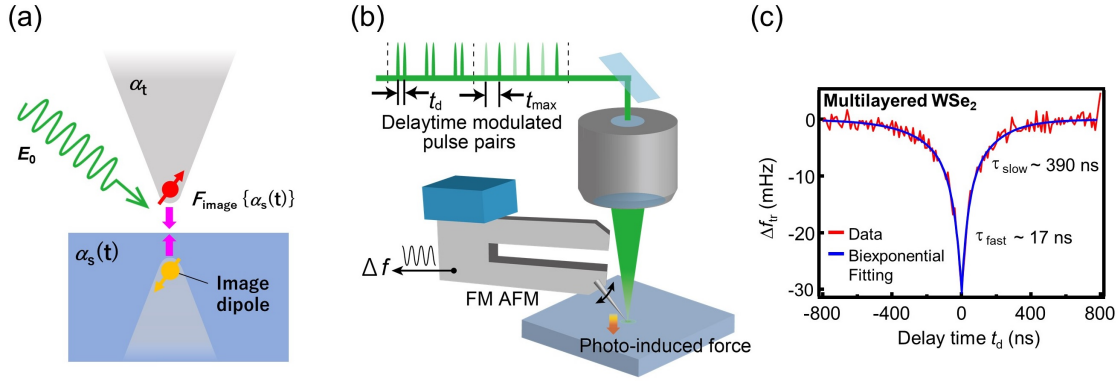


FIG. 4. (a) Dipole-dipole interaction mechanism.  $\alpha_t$ ,  $\alpha_s$ , and  $E_0$  are the complex effective polarizabilities of the tip and sample, the incident light electric field vector, respectively. (b) Schematic of tuning-fork-type time-resolved FM AFM setup. (c) Time-resolved signal obtained for a multilayer  $\text{WSe}_2$  sample and fitting results<sup>14</sup>.

realizing a higher-performance optical system enabling a wavelength-variable, externally controllable laser system with a smaller pulse width in the future. The development of easy-to-use optical systems and their applications to various scanning probe techniques will expand the capability of OPP-SPM techniques and contribute to a deeper understanding of various photo-induced phenomena.

## REFERENCES

- <sup>1</sup>Y. Terada, S. Yoshida, O. Takeuchi and H. Shigekawa, *Nat. Photonics* **4**, 869 (2010).
- <sup>2</sup>S. Yoshida, Y. Aizawa, Z.-H. Wang, R. Oshima, Y. Mera, E. Matsuyama, H. Oigawa, O. Takeuchi and H. Shigekawa, *Nat. Nanotechnol.* **9**, 588 (2014).
- <sup>3</sup>T. L. Cocker, V. Jelic, M. Gupta, S. J. Molesky, J. A. J. Burgess, G. De Los Reyes, L. V. Titova, Y. Y. Tsui, M. R. Freeman and F. A. Hegmann, *Nat. Photonics* **7**, 620 (2013).
- <sup>4</sup>M. Garg and K. Kern, *Science* **367**, 411 (2019).
- <sup>5</sup>S. Yoshida, Y. Arashida, H. Hirori, T. Tachizaki, A. Taninaka, H. Ueno, O. Takeuchi and H. Shigekawa, *ACS Photonics* **8**, 315 (2021).
- <sup>6</sup>Y. Arashida, H. Mogi, M. Ishikawa, I. Igarashi, A. Hatanaka, N. Umeda, J. Peng, S. Yoshida, O. Takeuchi and H. Shigekawa, *ACS Photonics* **9**, 3156 (2022).

- <sup>7</sup>S. Yoshida, M. Yokota, O. Takeuchi, H. Oigawa, Y. Mera and H. Shigekawa, *Appl. Phys. Express* **6**, 032401 (2013).
- <sup>8</sup>P. Kloth and M. Wenderoth, *Sci. Adv.* **3**, e1601552 (2017).
- <sup>9</sup>S. Yoshida, Y. Terada, R. Oshima, O. Takeuchi and H. Shigekawa, *Nanoscale* **4**, 757 (2012).
- <sup>10</sup>H. Mogi, Z. Wang, R. Kikuchi, C. Hyun Yoon, S. Yoshida, O. Takeuchi and H. Shigekawa, *Appl. Phys. Express* **12**, 025005 (2019).
- <sup>11</sup>K. Iwaya, M. Yokota, H. Hanada, H. Mogi, S. Yoshida, O. Takeuchi, Y. Miyatake and H. Shigekawa, *Sci. Rep.* **13**, 818 (2023).
- <sup>12</sup>J. Jahng, J. Brocious, D. A. Fishman, S. Yampolsky, D. Nowak, F. Huang, V. A. Apkarian, H. K. Wickramasinghe and E. O. Potma, *Appl. Phys. Lett.* **106**, 083113 (2015).
- <sup>13</sup>Z. Schumacher, A. Spielhofer, Y. Miyahara and P. Grutter, *Appl. Phys. Lett.* **110**, 053111 (2017).
- <sup>14</sup>H. Mogi, R. Wakabayashi, S. Yoshida, Y. Arashida, A. Taninaka, K. Iwaya, T. Miura, O. Takeuchi and H. Shigekawa, *Appl. Phys. Express* **17**, 015003 (2024).
- <sup>15</sup>H. Mogi, Y. Arashida, R. Kikuchi, R. Mizuno, J. Wakabayashi, N. Wada, Y. Miyata, A. Taninaka, S. Yoshida, O. Takeuchi and H. Shigekawa, *npj 2D Mater. Appl.* **6**, 72 (2022).
- <sup>16</sup>H. Mogi, Z. Wang, I. Kuroda, Y. Takaguchi, Y. Miyata, A. Taninaka, Y. Arashida, S. Yoshida, O. Takeuchi and H. Shigekawa, *Jpn. J. Appl. Phys.* **61**, SL1011 (2022).